Biology of Reproduction, 2021, 105(6), 1603–1616
https://doi.org/10.1093/biolre/ioab168
Research Article
Advance Access Publication Date: 14 September 2021

OXFORD

Research Article

Aurora A Kinase (AURKA) is required for male germline maintenance and regulates sperm motility in the mouse.

William C. Lester[1], Taylor Johnson[1,2], Ben Hale[1,2], Nicholas Serra[1,2], Brian Elgart[1], Rong Wang[1], Christopher B. Geyer[1,2] and Ann O. Sperry[1,*]

[1]Department of Anatomy and Cell Biology at the Brody School of Medicine, Greenville NC, USA and [2]East Carolina Diabetes and Obesity Institute, East Carolina University, Greenville NC, USA.

***Correspondence:** Department of Anatomy and Cell Biology, Brody School of Medicine, East Carolina University, Greenville, NC USA 27834, sperrya@ecu.edu

Received 12 August 2020; Revised 12 March 2021; Accepted 2 September 2021

Abstract

Aurora A kinase (AURKA) is an important regulator of cell division and is required for assembly of the mitotic spindle. We recently reported the unusual finding that this mitotic kinase is also found on the sperm flagellum. To determine its requirement in spermatogenesis, we generated conditional knockout animals with deletion of the *Aurka* gene in either spermatogonia or spermatocytes to assess its role in mitotic and postmitotic cells, respectively. Deletion of *Aurka* in spermatogonia resulted in disappearance of all developing germ cells in the testis, as expected, given its vital role in mitotic cell division. Deletion of *Aurka* in spermatocytes reduced testis size, sperm count, and fertility, indicating disruption of meiosis or an effect on spermiogenesis in developing mice. Interestingly, deletion of *Aurka* in spermatocytes increased apoptosis in spermatocytes along with an increase in the percentage of sperm with abnormal morphology. Despite the increase in abnormal sperm, sperm from spermatocyte *Aurka* knockout mice displayed increased progressive motility. In addition, sperm lysate prepared from *Aurka* knockout animals had decreased protein phosphatase 1 (PP1) activity. Together, our results show that AURKA plays multiple roles in spermatogenesis, from mitotic divisions of spermatogonia to sperm morphology and motility.

Key words: Aurora A kinase (AURKA), spermatogenesis, spermiogenesis, sperm motility, Protein phosphatase 1 (PP1).

Introduction

The mammalian sperm flagellum is required for sperm motility and normal fertility. It consists of four segments: (1) the connecting piece, containing the degenerate centriole at the base of the microtubule axoneme; (2) the midpiece, composed of mitochondria spirally arranged around the axoneme; (3) the principal piece; and (4) the end piece [1]. The principal piece comprises much of the length of the flagellum and contains the microtubule-based axoneme surrounded by seven outer dense fibers (ODFs); the ODFs are in turn encased by the fibrous sheath, a cytoskeletal structure unique to the sperm flagellum and located just beneath the sperm plasma membrane.

Aurora A kinase (AURKA) is a well-known mitotic regulator essential for centrosome maturation and separation to assemble the mitotic spindle at mitosis [2]. In addition to its role in mitosis, AURKA is found at the base of cilia in somatic cells, as well as the flagellum in *Chlamydomonas reinhardtti*, where it regulates flagella/cilia length [3, 4]. We previously reported that activated AURKA localizes to the mouse sperm midpiece and interacts with protein phosphatase 1 (PP1) in the testis [5]. PP1 is an important regulator of motility in the epididymis. Sperm are kept immotile in the caput epididymis by activated PP1 which counteracts the protein phosphorylation events necessary for motility [6].

Based on its role in cell division, location in cilia/flagella, and its association with PP1, we investigated the requirement for AURKA in male germ cell development and male fertility by deleting *Aurka* early during male germ cell development and then later, specifically

in spermatocytes. Our results reveal a requirement for AURKA in progression through mitosis, as expected, as AURKA-deficient spermatogonia were eliminated from the seminiferous epithelium. In contrast, mice with deletion of *Aurka* beginning in spermatocytes had increased germ cell apoptosis and reduced fecundity, with reduced testis weights and cauda epididymal sperm counts, and increased percentage of abnormal sperm. Surprisingly, the motility of the *Aurka* KO sperm was increased compared to the control. Coordinately, the activity of PP1, a modulator of sperm motility in the epididymis, was reduced in knockout sperm. We also identified AURKA-interacting proteins with demonstrated functions in sperm metabolism and flagellum structure. We conclude from these studies that, beyond its role in cell division, AURKA is required for spermiogenesis and controls sperm motility. We propose a model in which AURKA functions in sperm through both its association with proteins of the flagella and its regulation of PP1 to control normal sperm motility.

Materials and methods

Generation of experimental animals

All use of animals was approved and conducted in accordance with the International Animal Care and Use Committee of East Carolina University (NIH animal welfare assurance number A3469-01). *Aurka* spermatogonia KO (*Aurka* spgKO) mice were constructed by crossing adult female mice containing floxed *Aurka* alleles (*Aurka*$^{fl/fl}$, #017729, The Jackson Laboratory) with adult males expressing the *Ddx4*-Cre transgene (#006954, The Jackson Laboratory). *Aurka* spermatocyte KO (*Aurka* spcKO) mice were constructed by crossing *Aurka*$^{fl/fl}$ female mice with adult males containing one floxed allele and expressing the *Wisp3*-Cre transgene (#017685, The Jackson Laboratory). Floxed *Aurka* alleles and the Cre transgene were identified by PCR of tail tip DNA using the following specific primers: *Aurka* forward: TGAGTTGGAAAGGGACATGG; *Aurka* reverse: 5'-CTCCACCACCTTACTGTTGG-3′; *Ddx4*-Cre forward: 5'-CTAAACATGCTTCATCGTCGGTCC-3′, and *Ddx4*-Cre Reverse 5'-GGATTAACATTCTCCCACCGTCAG-3′; *Wisp3*-Cre forward: 5'-CGTAGGCTCCTCTTTTGCAC-3′;

Wisp3-Cre reverse: 5'-TGCAAGAAGGCTTCAGTGTG-3; Wisp3-Cre EGFP – r2 Reverse 5'-GAACTTCAGGGTCAGCCTGC-3. Cycling conditions for *Wisp3*: 94°C 2 min, then 35 cycles: 94°C 30 s, 65°C 30 s, 72°C 45 s. The deleted allele was confirmed using the following primers: forward primer DCF1: 5'-CCTGTGAGTTGGAAAGGGACATGGCTG-3′; reverse primer DCE6: 5'-GATGGAAACCCTGAGCACCTGTGAAAC-3′. Cycling conditions for deleted allele: 94°C 2′, then 35 cycles of 94°C 15 s, 68°C 30 s, 72°C 50 s, 72°C 5′ [7].

Identification of apoptotic spermatocytes

Indirect immunofluorescence was performed as previously described [8, 9] to determine whether *Aurka* deletion stimulated apoptosis in spermatocytes; this was accomplished by co-labeling cells with anti-cleaved PARP1 (a marker for apoptosis) and anti-SYCP3 (a marker for spermatocytes). Briefly, testes from control (defined as Fl/+; Cre and Fl/+; no Cre) and *Aurka* spcKO mice (defined as Fl/Fl; Cre) were fixed in 4% paraformaldehyde and embedded in O.C.T. Blocking and antibody incubations of 5 µm sections were performed using 1× PBS containing 3% BSA plus 0.1% Triton X-100. Strict washes using 1× PBS plus 0.1% Triton X-100 followed each antibody incubation. All sections were blocked for 30 min at room temperature prior to antibody incubations for 1 h at room temperature. Black 1.5 ml tubes and non-luminescent containers were implemented to minimize light exposure during staining of tissues. Primary antibody was omitted from adjacent sections for use as a negative control. Antibodies used were anti-cleaved PARP1 (1: 100 dilution; Cat# 94885S, Cell Signaling Technology), anti-SYCP3 (1: 250 dilution; Cat# ab205846, Abcam), and Alexa Fluor-555 donkey anti-rabbit (1: 250 dilution; Cat# A31572, Thermo Fisher Scientific). Coverslips were mounted in 50% 1X PBS: 50% Fluoroshield with 4′,6-diamidino-2-phenylindole (DAPI; enQuire BioReagents) and images were obtained using a Zeiss Celldiscoverer7. For quantitation, the negative control slides were used to calibrate thresholds. Counting was performed on approximately 100 seminiferous tubules from each mouse (n = 3–4 mice per group). Data reflect: (1) the number of cPARP1+/SYCP3+ cells (apoptotic spermatocytes) divided by the perimeter of the seminiferous tubule (units in cells/mm); and (2) the percentage of tubules containing apoptotic spermatocytes. Fluorescent phalloidin (Alexa Fluor-635; 1:1000 dilution; Cat# A34054, Thermo Fisher Scientific) was included to outline each tubule. Statistical analyses were performed using Student's t-test. Three control and three KO mice were used in experiments.

Motility assessment. Sperm were collected from cauda epididymides of spcKO and control mice as previously described [10]. Briefly, adipose and connective tissue were carefully removed, and cauda epididymides were rinsed in prewarmed PBS, then transferred to a 12-well plate containing 1 ml/cauda of prewarmed HTF media (human tubal fluid, 101.6 mM NaCl, 4.7 mM KCl, 0.37 mM KH_2PO_4, 0.2 mM $MgSO_4.7H_2O$, 2 mM $CaCl_2$, 2.78 mM glucose, 0.33 mM pyruvate, 4 mM $NaHCO_3$, 21 mM HEPES, 21.4 mM lactate, and 5 mg/ml BSA), which had been prewarmed to 37°C under 5% CO_2. Using a dissecting microscope, four to six cuts were made in the cauda epididymis to allow motile sperm to swim out into the media for at least 15 min at 37°C under 5% CO_2. Sperm were then diluted 1:20 in HTF media in a 6-well plate. A total of 10 random fields were captured per timepoint per treatment. Motility was assessed using Computer Assisted Sperm Analysis (CASA; Hamilton Thorne). We used default Hamilton Thorne Mouse 2 settings, which included capturing 90 frames in each field, and slow sperm were counted as motile. Default mouse 2 settings were as follows: 60 frames per second, minimum contrast = 30, minimum cell size = 4 pixels, cell size = 13 pixels, cell intensity = 75, progressive cells were defined as path velocity (VAP) > 50 µ/s and straightness >50%, and slow cells were defined where VAP cutoff = 10 µ/s and VSL cutoff = 0 µ/s. Default static gates are as follows: static intensity gate minimum = 0.10, static intensity gate maximum = 1.52, static size gate minimum = 0.13, static size gate maximum = 2.43, static elongation gate minimum = 5, static elongation gate maximum = 100. Statistical analyses were performed using Student's t-test.

Breeding trial

Males were housed with 1 homozygous fl/fl; no Cre female for 120 days after both had reached 60 days of age (KO n = 6, control n = 9). Statistical analyses were performed using JMP Version 13.1. Data were expressed as mean ± SEM and analyzed by using an equal variance two-tailed t-test setting $P \leq 0.05$ to determine significant difference of the means of the AURKA $^{-/-}$ and control (heterozygous$^{+/-}$) mating pairs.

Immunoblot analysis

Mouse sperm were isolated from cauda epididymides as described above, washed in 1X PBS, concentrated by centrifugation, and resuspended in RIPA buffer with 1% PMSF and 1% HALT protease cocktail (78,446, ThermoFisher). The sperm suspension was sonicated on ice six to eight times for 2 s each at output level 2 (Branson Sonifier 250), and the insoluble fraction removed by centrifugation at 16 000xg at 4°C for 10 min. *Forty micrograms of the soluble protein extract from the sperm lysate were boiled in SDS buffer for 5 min,* separated by 10% SDS-polyacrylamide gel electrophoresis and transferred to polyvinylidene difluoride membranes. Membranes were blocked in 5% nonfat dry milk in TTBS (100 mM Tris, pH 7.5, 150 mM NaCl, 0.1% Tween 20) and incubated with primary antibodies (AURKA, 1:200, PA5–34700; Thermo Fisher Scientific), diluted in blocking buffer and incubated overnight at 4°C. Membranes were washed three times for 5 min in TTBS and incubated with horseradish peroxidase-conjugated secondary antibodies (donkey anti-rabbit, 1:2500, Jackson ImmunoResearch Laboratories, donkey anti-mouse, 1:2500, Pierce) for 1 h at RT in blocking buffer. Following incubation, membrane was washed three times for 5 min. Detection of protein targets was done using SuperSignal West Pico Chemiluminescent Substrate kit (Pierce).

Identification of germ cell populations. Fluorescent staining was performed as previously reported [11] to determine the presence of specific germ cell types in mice and the colocalization of AURKA+ cells with germ and somatic cell markers. PFA fixed testes obtained from two CD-1 male mice were washed in 1X PBS and incubated in 30% sucrose overnight in 4°C. Testes were then frozen in O.C.T. and sectioned at 5 µm. Sections were incubated in blocking solution (1X PBS + 3% BSA + 0.1% Triton X-100) for at least 30 min at room temperature. Thereafter, primary antibodies were diluted with blocking solution at appropriate ratios (TRA98, Abcam AB82527, 1:1000; GATA4, Cell Signaling 36966S, 1:400, KIT, R&D Systems, AF1365 1:1000, SYCP3, Abcam ab205846, 1:250 dilution) and incubated on tissue sections for 1 h at room temperature. One section per slide incubated in blocking solution absent of antibodies served as an experimental negative control. Following 15 min in washing solution (1X PBS + 0.1% Triton X-100), sections were incubated in blocking solution containing the corresponding fluorescent secondary antibody (488 Donkey Anti-Rabbit, Invitrogen A21206, 1:500; 594 Donkey Anti-Rat, Invitrogen A21209, 1:500) and/or a primary antibody pre-conjugated with a desired fluorophore for 1 h at room temperature. Washing steps were performed as previously described, and coverslips were mounted in 50% 1X PBS/ 50% DAPI with mounting medium (EnQuire BioReagents). All incubating and washing steps were performed in humid, opaque containers and solutions with fluorescent antibodies were prepared in black tubes to minimize light exposure throughout the experiment. Primary antibody was omitted from adjacent sections for use as a negative control. Stained sections were imaged using a Fluoview FV1000 laser scanning confocal microscope (Olympus America). For imaging purposes, control slides with no primary antibody were used to calibrate thresholds. Two control and two *Aurka* spgKO mice were used to verify expression.

Sperm immunostaining

The cauda epididymides from Aurka spcKO or control male mice were carefully removed, placed in prewarmed phosphate buffered saline, and four to six cuts were made to allow sperm to swim out for 10 min in a 37°C water bath. The resulting sperm suspension was smeared onto glass slides for staining. Sperm density was verified under a light microscope, and slides were air-dried for at least 30 min at room temperature. Once completely dry, sperm were fixed in cold 4% PFA for 10 min and then stored at 4°C. Before immunostaining, TBST was used to remove residual PFA. Sperm were blocked in 3% BSA for 1 h at room temperature, and then stained with antibodies against AURKA (1:50, PA5–34700; ThermoFisher), and TPX2 (1:200, MA1–802; Thermo Fisher Scientific). Vectashield (Vector Laboratories) containing DAPI was used for mounting coverslips and visualization of DNA. Fluorescently labeled sperm were observed with a Nikon E600 fluorescence microscope fitted with the appropriate filters at 100X and 400X magnification and images captured with an Orca II CCD camera (Hamamatsu).

Coomassie staining

Sperm were isolated from cauda epididymides of *Aurka* spcKO male mice as described, fixed in 4% paraformaldehyde for 15 min then collected by centrifugation and rinsed with PBS. Sperm were spread on Superfrost Plus slides and stained for 10 min in Coomassie solution (50% methanol, 0.05% Coomassie Brilliant Blue-R250, 10% acetic acid), then rinsed in water and coverslipped. Sperm were visualized with an Revolve 4 Upright, Inverted Microscope and images captured with a CMOS digital camera (ECHO) at 20X magnification.

Immunoprecipitation. For identification of AURKA-associated proteins, mouse sperm were isolated from cauda epididymides and sperm lysate prepared as described above. AURKA antibody (IHC-00703, Bethyl Antibodies) was coupled to Dynabeads at 10 µg/mg (14311D, ThermoFisher) according to manufacturer's instructions. Sperm lysates (450 mg) were incubated with coupled beads overnight with rotation at 4°C. Beads were washed five times in buffer, collected by centrifugation, and the beads with associated proteins were subject to on-bead digestion followed by mass spectrometry at the UNC Michael J Hooker Proteomics Core (Chapel Hill, NC). Immunoprecipitation was verified by blotting of a duplicate sample with the AURKA antibody. The negative control was precleared lysate without antibody.

Proteomic methods

Protein complexes bound to beads were subjected to on-bead trypsin digestion as previously described [12]. After digestion, beads were collected, the supernatant removed, then the beads were washed twice with LC/MS grade water. The supernatants were combined, desalted, and dried. The peptide samples analyzed by LC/MS/MS using an Easy nLC 1200 coupled to a QExactive HF mass spectrometer (Thermo Scientific). Samples were injected onto an Easy Spray PepMap C18 column (75 µm id × 25 cm, 2 µm particle size) (Thermo Scientific) and separated over a 120 min period. The gradient for separation consisted of 5–40% mobile phase B at a 250 nl/min flow rate, where mobile phase A was 0.1% formic acid in water and mobile phase B consisted of 0.1% formic acid in 80% ACN. The QExactive HF was operated in data-dependent mode where the 15 most intense precursors were selected for subsequent fragmentation. Resolution for the precursor scan (m/z 350–1600) was set to 120 000 with a target value of 3×10^6 ions. MS/MS scans resolution was set to 15 000 with a target value of 5×10^4 ions, 60 ms max injection time. The normalized collision energy was set to 27% for HCD. Dynamic exclusion was set to 30 s,

peptide match was set to preferred, and precursors with unknown charge or a charge state of 1 and ≥ 7 were excluded. Data analysis was conducted as follows. Raw data files were processed using Proteome Discoverer version 2.1 (Thermo Scientific). Peak lists were searched against a reviewed Uniprot mouse database appended with a common contaminants database. The following parameters were used to identify tryptic peptides for protein identification: 10 ppm precursor ion mass tolerance; 0.02 Da product ion mass tolerance; up to two missed trypsin cleavage sites; carbamidomethylation of Cys was set as a fixed modification; oxidation of was set as a variable modification.

Scaffold (version 4.7.3, Proteome Software) was used to validate MS/MS based peptide and protein identifications, and to provide relative quantitation. Peptide identifications were accepted if they could be established at greater than 95% probability to achieve an FDR less than 0.1% by the Scaffold Local FDR algorithm. Protein identifications were accepted if they could be established at greater than 99.0% probability and contained at least two identified peptides. Relative quantitation was performed using the calculated quantitative values (spectral counts) within Scaffold.

Phosphatase assay

PP1 activity was detected using a RediPlate™ 96 EnzChek® Serine/Threonine Phosphatase Assay Kit as per manufacturer's instruction (Invitrogen). Sperm lysate used for phosphatase assay was prepared from control and *Aurka* spcKO sperm as described above except for the absence of phosphatase inhibitor cocktail.

Results

AURKA was primarily expressed in spermatids in the seminiferous epithelium

AURKA is a mitotic kinase critical for centrosome maturation and mitotic spindle formation [13]. We used three approaches to define the expression pattern of AURKA in the mouse testis: (1) localization of AURKA during testis development, (2) localization of AURKA in different seminiferous epithelium stages, and (3) costaining of AURKA with germ- and somatic- cell specific markers. AURKA expression was first seen at day 22 postpartum (P22) when round spermatids appear in the seminiferous epithelium (Figure 1). To determine the seminiferous tubule stages containing AURKA positive cells, wild type testis sections were stained for lectin, AURKA, and TRA98 (Figure 2). AURKA was detected in stages I–VI, (round spermatids, Figure 2A-A', B-B′) and stage VIII-IX (elongating spermatids) (Figure 2, C-C′, D-D′). AURKA signal was reduced in condensing spermatids in stages X–XII (Figure 2 E–E'). We then colocalized AURKA with cell type specific markers in adult testis (Figure 3). We saw no overlap of AURKA staining with the acrosome (A-A') or markers for spermatocytes (SYCP3, Figure 3B-B') progenitor spermatogonia (PLZF, Figure 3C), differentiating spermatogonia (KIT; Figure 3D), or Sertoli cells (GATA4, Figure 3E). Negative control with primary antibody incubated with the *Aurka* spg KO is shown in Figure 3F.

AURKA is required for germline survival

Whole-body deletion of *Aurka* in mice caused embryonic lethality [14]. To determine its specific requirement in spermatogenesis, we first created a male germ cell-specific deletion by crossing female mice homozygous for a floxed *Aurka* allele with males expressing the *Ddx4*-Cre transgene, which is active in prospermatogonia in the fetal testis as early as embryonic day E15.5 [15]. Due to the requirement of AURKA in mitosis, we predicted these spermatogonia KO (*Aurka* spgKO) male mice would lack germ cells. Compared to littermate controls, *Aurka* spgKO animals were viable and apparently healthy, but their testes were significantly smaller and their epididymides were devoid of sperm (Figure 4A-B, data not shown). Histological analyses of their testes revealed that, in comparison to littermate controls (Figure 4C), testes of *Aurka* spgKO mice lacked germ cells and exhibited Sertoli cell-only (SCO) tubules (Figure 4D-E). To confirm this finding, we stained with antibodies specific for all germ cells (TRA98/GCN1) and Sertoli cells (GATA4) (Figure 4G-H). Only Sertoli cells were observed in the seminiferous epithelium of *Aurka* spgKO mice (Figure 4H).

Deletion of AurkA in spermatocytes reduced testis size and decreased fecundity

We next explored the specific requirement for AURKA later in spermatogenesis by crossing *Aurka* floxed mice with those carrying *Wisp3*-Cre, which mediates deletion early in prophase of meiosis I (spermatocyte conditional, *Aurka* spcKO mice) [16]. The timing of *Aurka* deletion in these mice was precisely determined in our animals by PCR analysis of DNA obtained from the testis of prepuberal animals from P12 to P18. Gene deletion was first visible at P16, a time containing meiotic stages from preleptotene to pachytene spermatocytes (Figure 5A); however, recombination was highest at P18. Gene deletion resulted in almost complete elimination of AURKA in sperm and 90% reduction in total testis normalizing to ACTB (Figure 5B). Although body weights were indistinguishable from controls, testes of adult *Aurka* spcKO mice were ~30% smaller (Figure 5C, E). This reduced size indicated loss of cellularity, typically affecting the germline. Consistent with this, *Aurka* spcKO mice had a ~5-fold reduction in cauda epididymal sperm, suggesting impaired spermatogenesis (Figure 5F). The reduction in sperm count was due to decreased sperm and not due to a motility defect because the value did not change significantly when sperm count was measured without a swim out step. Analysis of testis histology revealed that, compared to control testes (Figure 5G-G'), adult *Aurka* spcKO testes contained tubules with complete spermatogenesis (Figure 5H-H').

We next determined whether the smaller testis size and reduced sperm counts in *Aurka* spcKO mice negatively affected their fertility. We performed breeding trials in which control *Aurka* spcKO male mice (spcKO n = 6, control n = 9) were co-housed with a wild type (WT) female for 4 month. Although the number of litters were similar (Figure 5D), the average litter sizes were significantly reduced in *Aurka* spcKO x WT breeding pairs (n = 4.2 pups/litter) as compared to littermate controls (n = 6 pups/litter) (Figure 5D). We therefore conclude that AURKA is required for normal male fertility.

Deletion of AURKA in spermatocytes increased apoptosis

The reduced testis size and histology of *Aurka* spcKO testis suggested an increased level of apoptosis in these animals. Preliminary studies demonstrated that programmed cell death was confined to germ cells (data not shown). We then measured apoptosis specific to spermatocytes by costaining with cPARP1 and SYCP3, a spermatocyte marker (Figure 6 A-B′). Testes from *Aurka* spcKO animals displayed as much as 3-fold higher levels of apoptosis in spermatocytes compared to controls (B-B′), as judged by cleaved (c)-PARP1 staining (Figure 6C) compared to controls (Figure 6D). These differences are displayed both as the number of spermatocytes per tubule volume (Figure 6C,

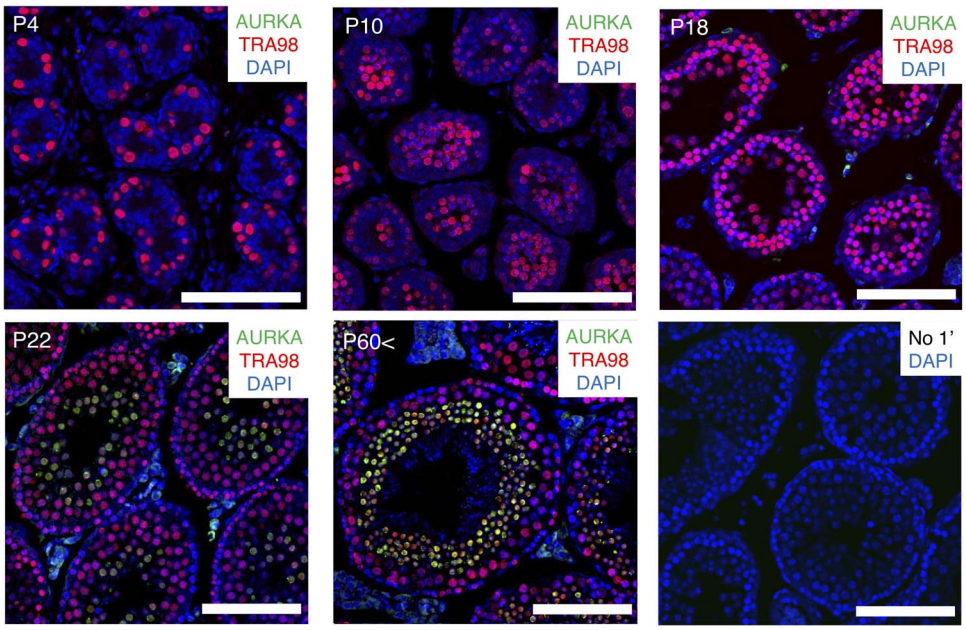

Figure 1. ***AURKA expression was first detected when spermatids appear in the developing testis.*** AURKA was colocalized with the pan-germ cell marker TRA98 in testis sections from wild-type animals at the indicated days post-partum (P). AURKA staining first became visible at P22. No primary antibody control with DAPI (blue) is shown in bottom right. Scale bar = 100 μm.

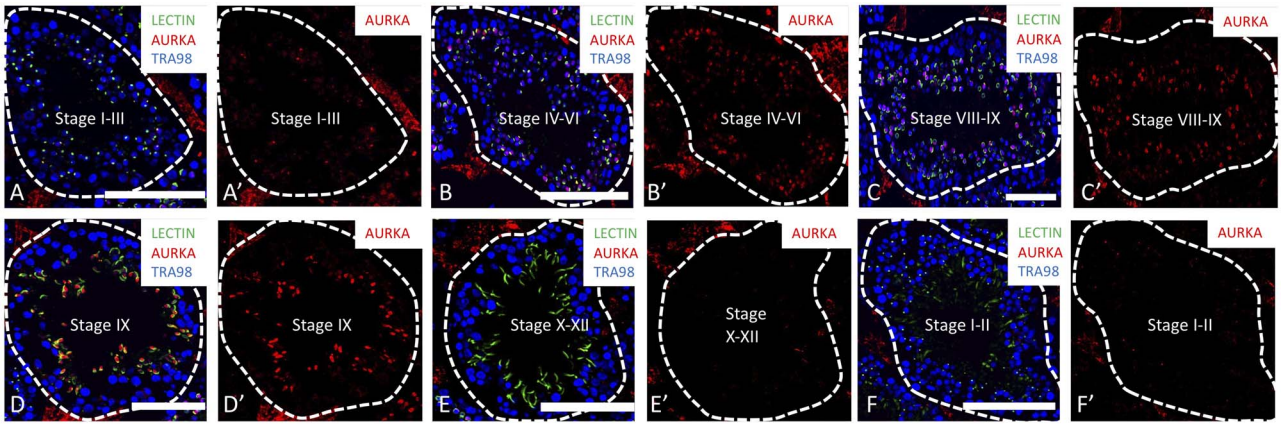

Figure 2. ***AURKA was expressed in seminiferous tubule stages containing round and elongating spermatids.*** Paraffin sections of wild-type testes were stained with lectin (green) for acrosomes, AURKA (red) and TRA98 (blue) for germ cells. AURKA stained seminiferous tubule stages containing spermatids, with most prominent staining at stages IV–VI (round spermatids) and stage IX (elongating spermatids). Condensing spermatids in stage X–XIII showed diminished staining. Scale bars = 100 μm.

$P = 0.004$) and percentage of tubules with apoptotic spermatocytes (Figure 6D, $P = 0.007$).

Aurka spcKO sperm lack Aurora A in the flagella midpiece

We previously reported that active AURKA was strongly localized to the midpiece of the flagellum and exhibited a weaker, punctate staining on the sperm principal piece [5]. That result was confirmed here (Figure 7A, C-C'), and we found AURKA was undetectable on flagella of *Aurka* spcKO sperm (Figure 7B) compared to controls. Additionally, spcKO mice containing the deleted allele and progeny of these mice had complete penetrance of the deleted allele (Supplemental Figure S1).

Aurka KO mice have sperm with abnormal morphology

We next assessed sperm morphology by scoring abnormal heads/flagella in sperm from *Aurka* spcKO and control animals. To do this, we scored abnormal heads (either multiple or malformed), abnormal tails (multiple), curved midpieces, and flagella bent or folded at the annulus in *Aurka* spcKO and control sperm. *Aurka* spcKO mice had an approximate ~3-fold increase in morphologically abnormal sperm compared to littermate controls (Figure 7J). Abnormalities were significantly increased in sperm from the *Aurka* spcKO including sperm curled at the midpiece (Figure 7E, $P \leq 0.00001$), multiple tails (Figure 7F, H, $P = 0.04$), malformed heads (Figure 7F, $P = 0.03$), flagella folded or bent at the annulus (Figure 7G-I, arrows, $P \leq 0.00001$). Sperm midpiece curling was the

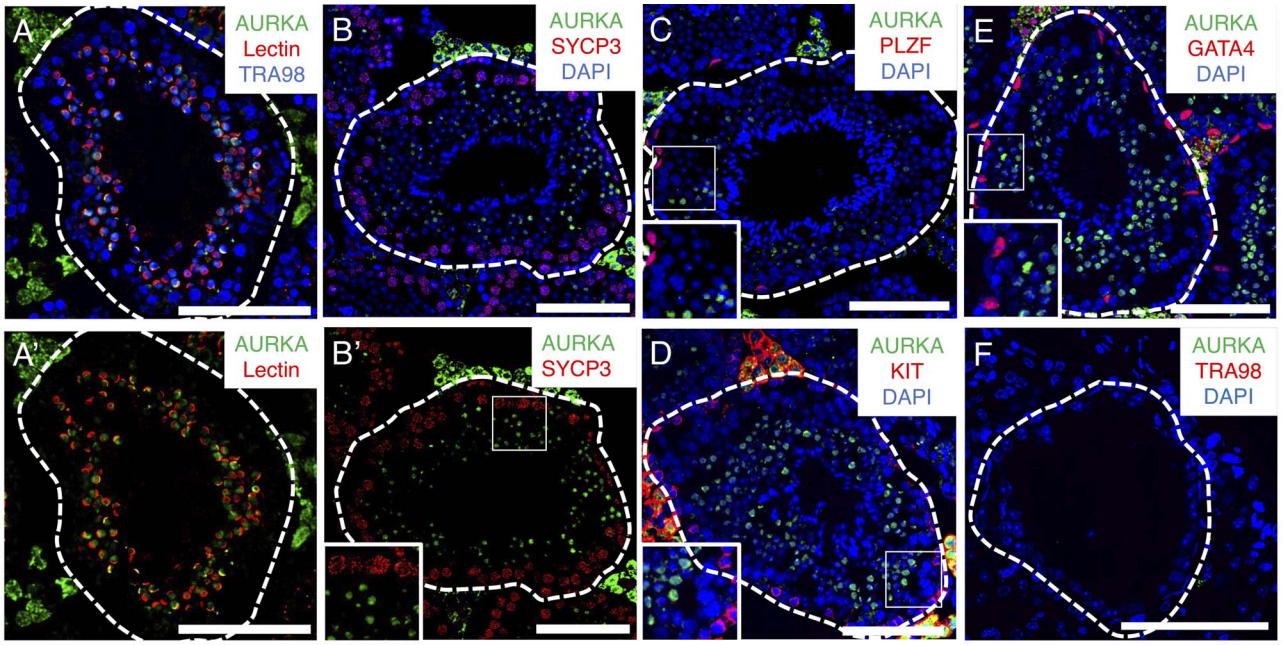

Figure 3. ***AURKA does not colocalize with spermatogonia, spermatocytes, or Sertoli cells.*** Indirect immunofluorence (IIF) was performed on frozen sections testis from wild-type animals stained for AURKA (green) and the indicated cell type specific markers (red): (A-A') lectin, (B, B') SYCP3, (C) PLZF, (D)KIT, and GATA4 (E). (F) Staining of testis section taken from *Aurka* spgKO animal stained with AURKA (green), TRA98 (red), and DAPI (blue). Scale bar = 100 μm.

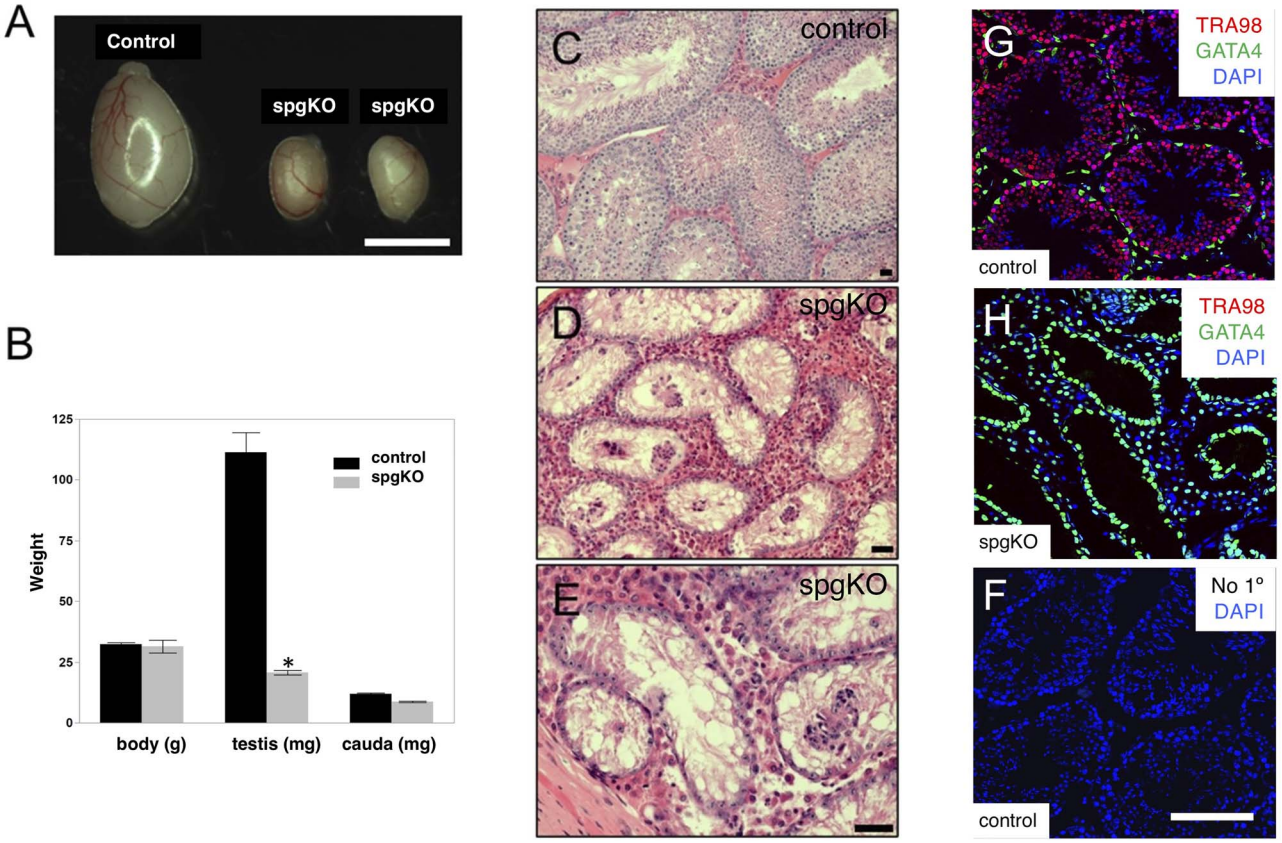

Figure 4. ***Germ cells were absent in the spgKO testis.*** (A) Images of representative testis of control and spgKO testis. (B) Relative weights of body, testis, and cauda epididymis of control and spgKO mice. Control (C) and mutant (D-E) testis sections stained with H&E. IIF was performed to determine the presence of germ cells within tubules of *Aurka* spgKO testis. (G) Control testes stained with TRA98 (red), GATA4 (green), and DAPI (blue). (H) spgKO stained with TRA98 (red), GATA4 (green), and DAPI (blue). (F) No primary/DAPI-only staining of a WT testis section. Scale bar = 100 μm.

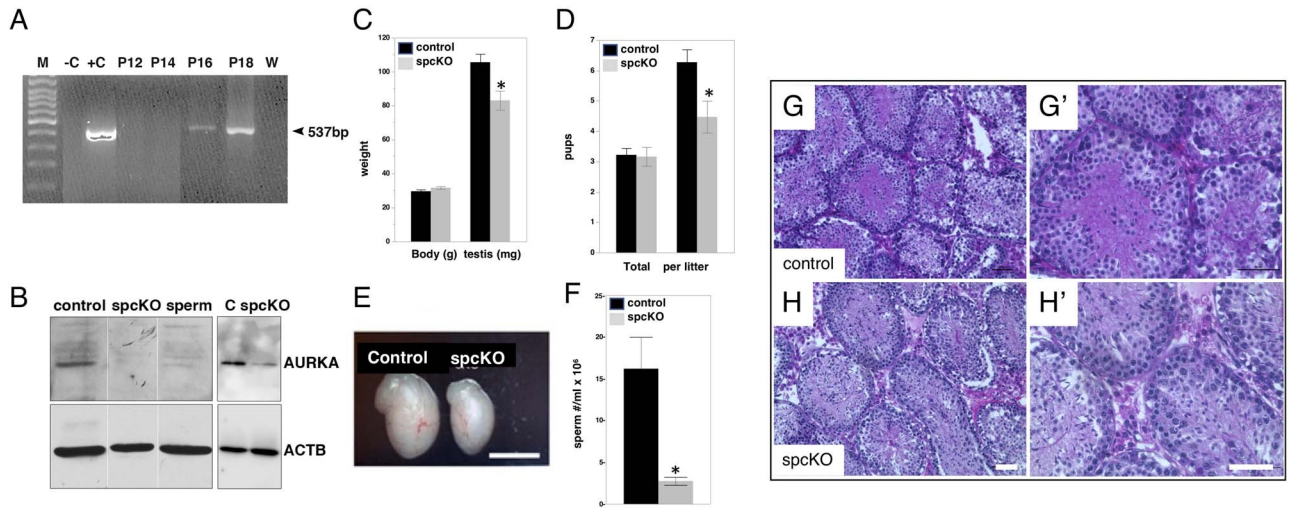

Figure 5. ***Deletion of Aurka in spermatocytes reduced testis size and decreased fecundity.*** (A) PCR analysis of *Aurka* deletion in animals at the indicated days after birth using 200 ng DNA per reaction using the cycling conditions described in Materials and Methods. The presence of the deleted allele is indicated by a 567 bp band (B) Western blot of sperm and testes lysates from control and spcKO probed for AURKA and ACTB. (C) Relative weights of control and *Aurka* spcKO body and testis ($P < 0.05$). (D) *Aurka* spcKO showed reduced litter size per pregnancy among the approximately same number of litters ($P \leq 0.05$) (E) Images of representative testes from a littermate control and *Aurka* spcKO. (F) Comparison of sperm numbers between control and *Aurka* spcKO mice. Histological sections stained with H&E from control (G-G′) and *Aurka* spcKO (H, H′) testis shows normal histology, complete with supporting cells and multiple generations of germ cells. Images were taken at 200X (G-H) or 400X (G′-H′). Scale bar = 50 μm.

most abundant malformation (63%) followed by bent tails (29%), head malformations (6%), and multiple tails (2%) (Figure 7J).

Aurka spcKO mice exhibited increased sperm motility

Based on the significant increase in abnormal sperm in the *Aurka* spcKO, we predicted that these sperm would be less motile. We utilized CASA to quantify specific sperm motility parameters in sperm from control and *Aurka* spcKO animals (Figure 8). In fact, although their total motility was not significantly increased (Figure 8A), the progressive motility of *Aurka* spcKO sperm increased by 25% compared to control ($P = 0.04$) (Figure 8B). Other parameters reflecting velocity including path velocity (VAP) and curvilinear velocity (VCL) were also significantly increased in the mutant (Figure 8E, $P = 0.01$). Straight line motility (VSL) was also increased in the mutants, but the difference was not statistically significant ($P = 0.06$). Other motility parameters were not significantly different for *Aurka* spcKO sperm compared to control (Figure 8E).

PP1 activity is reduced in spcAurka KO sperm

We have previously shown that AURKA interacts with PPP1CC in the developing testis, consistent with the proposed role for AURKA in regulating PPP1CC in spermatids and sperm [5]. To determine if AURKA regulates PP1 in sperm and if PP1 activity was altered in the *Aurka* spcKO knockout, we compared the PP1 activity in sperm lysate from *Aurka* spcKO sperm with that of control animals. PP1 activity was significantly reduced in sperm lysate from *Aurka* spcKO sperm compared to controls (Figure 9, $P = 0.0004$).

The sperm AURKA complex is enriched in mitochondrial proteins, proteins of the fibrous sheath, microtubule binding proteins, and metabolic proteins

We next sought to identify AURKA binding partners and potential downstream targets of AURKA in the sperm flagellum. Proteins associated with AURKA were immunoprecipitated from sperm lysates along with AURKA and then identified by mass spectrometry. No peptides were identified in the no antibody control. The proteins identified in this screen were clustered into functional categories using DAVID (the Database for Annotation, Visualization and Integrated Discovery) to query multiple databases [17, 18]. We identified mitochondrial proteins, proteins of the fibrous sheath, microtubule binding proteins, and metabolic enzymes as enriched in the immunoprecipitate (Table 1). Of the 166 proteins in our screen, the most enriched category was mitochondrial proteins, consistent with localization of AURKA to the midpiece of the flagella where mitochondria reside (Figure 7C'). Notably, components of the F_1 and F_2 ATPase were identified in our screen. Proteins of the fibrous sheath were also enriched in the identified binding proteins including two important calcium binding proteins of the fibrous sheath—"fibrous sheath CABYR-binding protein" (FSCB) and "calcium-binding tyrosine phosphorylation regulated protein" (CABYR) (Table 2).

Another interesting AURKA binding protein identified in our screen was PKA anchoring protein (AKAP4). Several members of the tektin (TEKT) family of microtubule-stabilizing proteins (TEKT2, TEKT3, and TEKT5) were also associated with AURKA. Using the phosphorylation site prediction program GPS5.0 [19], we searched the AURKA-associated proteins for predicted AURKA phosphorylation sites and found that each of these proteins contained high confidence predicted phosphorylation sites for AURKA (Table 3). Our screen also identified the metabolic proteins phosphoglycerate kinase 2 (PGK2) and nucleoside diphosphate kinase 7 (NPK7). Both proteins are associated with the sperm flagellum, although in the principal piece.

Discussion

In somatic cells, AURKA is an essential component of the centrosome and is required for formation of the mitotic spindle through an association with spindle fibers. AURKA regulates mitosis by

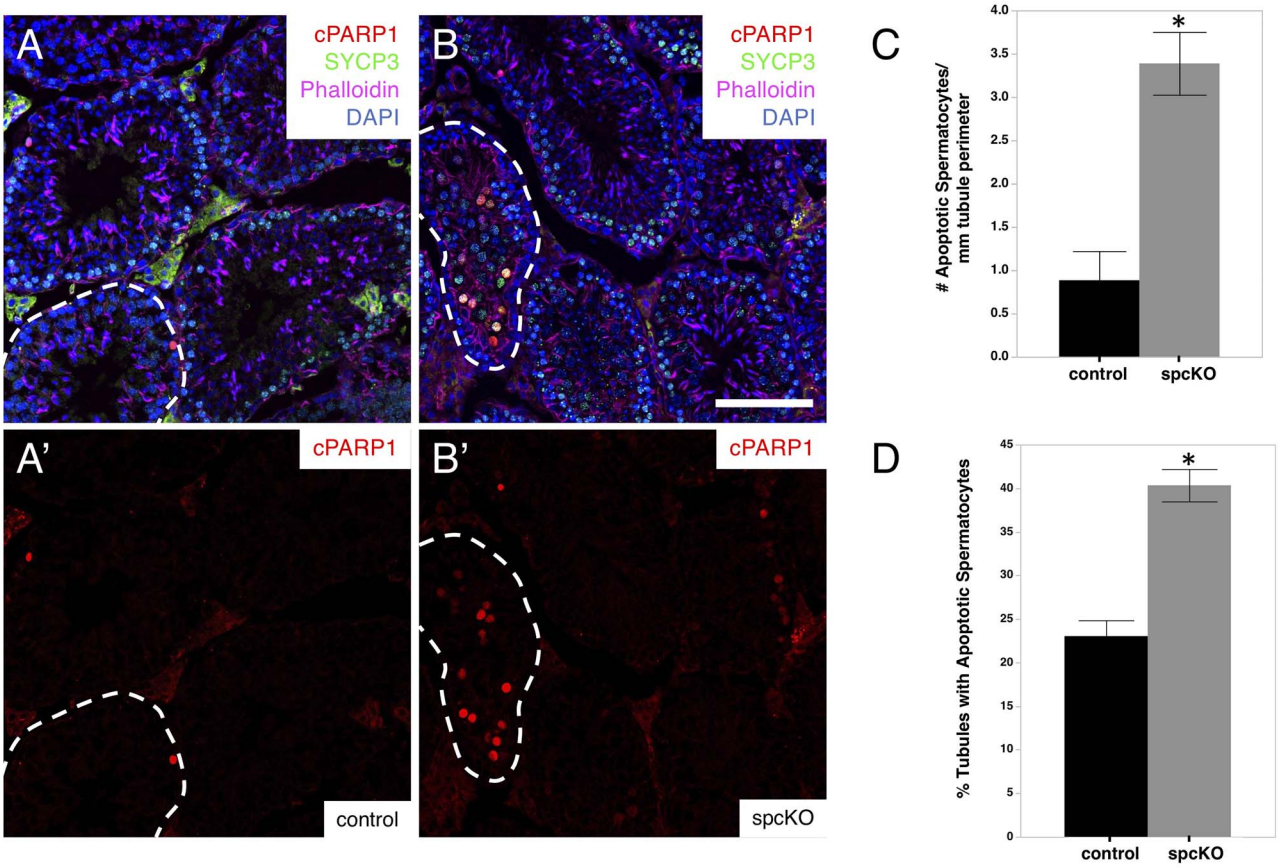

Figure 6. ***Deletion of Aurka in spermatocytes increased apoptosis.*** IIF was performed with testis sections from postnatal day (P) 35 control mice (A-A′) or *Aurka* spcKO mice (B-B′) Five-micrometer sections were used for detection of cPARP1 (red) and SYCP3 (green). Phalloidin (magenta) was used to visualize the outlines of tubule cross-sections and DAPI labeled nuclei (blue) (A′ and B′) the isolated red channel for (A and B, cPARP). (C) Testis tubule cross-sections containing spermatocytes (SYCP3+ cells) positive for cPARP1 were counted, and their numbers were normalized to the tubule perimeter (in mm). Error bars are SD. (D) The number of tubule cross-sections containing apoptotic spermatocytes was divided by the total number of tubule cross-sections counted (approximately 100 cross-sections per mouse). Error bars are SD and $P < 0.01$ vs control. Scale bar = 100 µm.

Table 1. ***The AURKA complex was enriched in mitochondrial proteins, flagellar proteins, and metabolic proteins.*** The list of proteins identified by mass spectrometry was entered into DAVID (the Database for Annotation, Visualization, and Integrated Discovery), a batch annotation and gene-GO term enrichment analysis tool. The output displays the total gene count in each class, the calculated *P* value and the relative enrichment score calculated from all members of the protein cluster.

Protein cluster	Class	Count	P value	Enrichment score
1	Mitochondrion	45	1.1×10^{-13}	12.5
	Mitochondrial inner membrane	20	8.2×10^{-11}	
	Mitochondria transit peptide	23	1.2×10^{-10}	
2	Sperm fibrous sheath	7	4.3×10^{-10}	4.89
	Tektin	5	9.9×10^{-9}	
	Motile cilium	10	2.8×10^{-8}	
	Sperm principal piece	7	3.1×10^{-8}	
	Cilium	14	6.5×10^{-8}	
	Cell projection	15	8.6×10^{-4}	
	Microtubule	9	3.1×10^{-3}	
	Cytoskeleton	13	1.2×10^{-1}	
3	Metabolic process	16	1×10^{-6}	3.97
	Mitochondrial matrix	9	8.2×10^{-5}	
	Catalytic activity	12	7.1×10^{-4}	

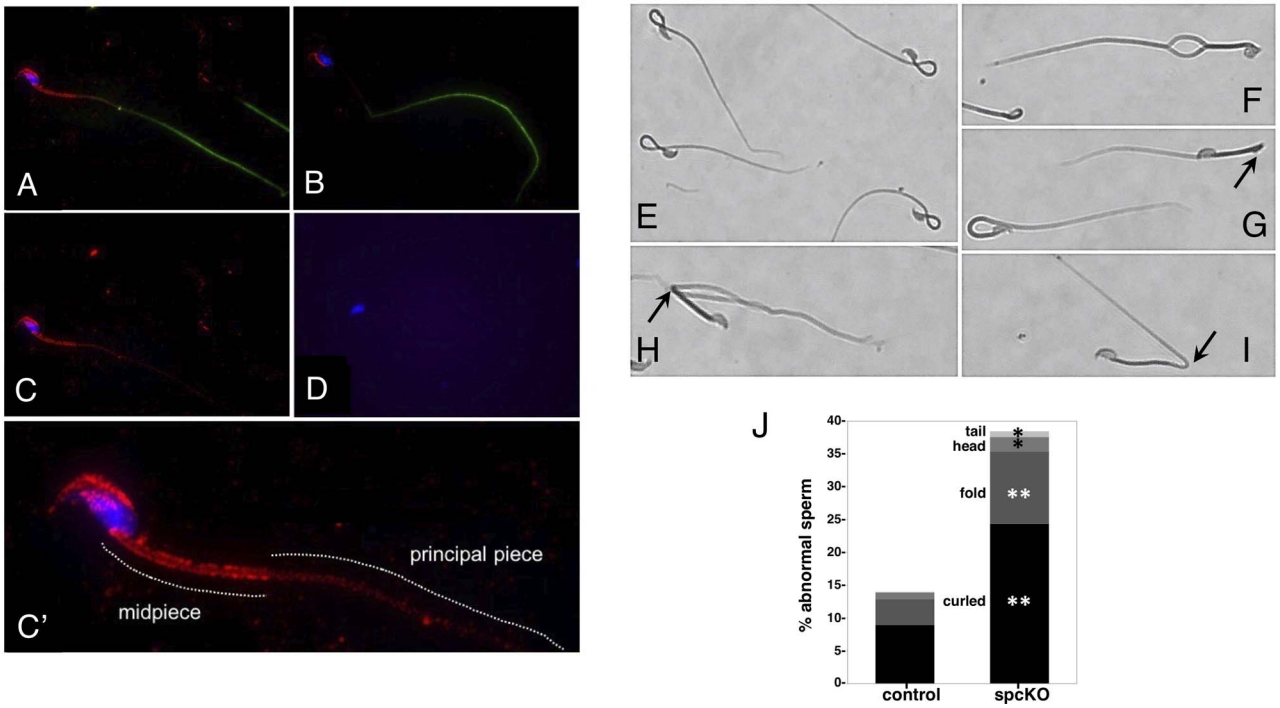

Figure 7. ***Aurka spcKO mice exhibited sperm with abnormal morphology*** (A) Sperm from cauda epididymides of a control mouse were stained with antibodies to AURKA (red) and TPX2, a microtubule binding protein (green). (B) Sperm from the cauda epididymides of an *Aurka* spcKO mouse were stained with antibody to AURKA (red) and TPX2 (green) showing lack of staining in the flagella. (C, C′) Red channel of sperm shown in A (D is no antibody control) and the midpiece and principal piece are indicated by dashed lines. (E-I) Representative images of abnormal sperm seen in the *Aurka* spcKO mice (J) Graphical representation of the percent abnormal sperm in the *Aurka* spcKO versus control. *$P \leq 0.05$, **$P \leq 0.00001$.

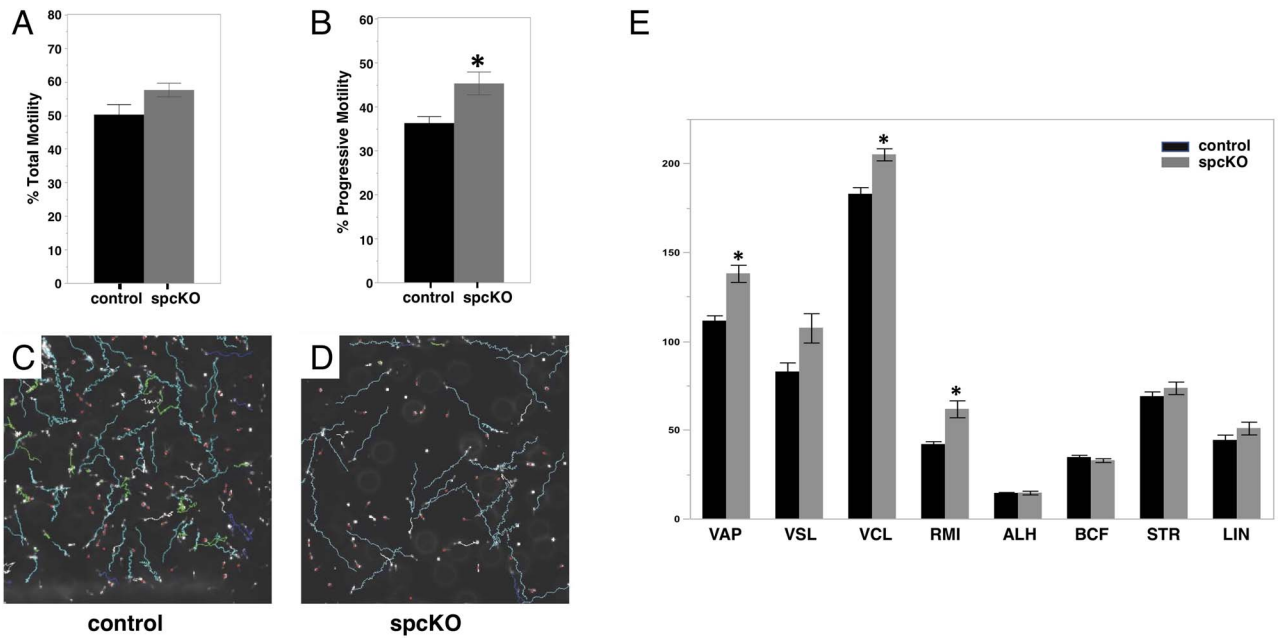

Figure 8. *Aurka spcKO sperm exhibited increased progressive motility.* Sperm were isolated from the cauda epididymides of *Aurka* spcKO and control and motility parameters were analyzed by CASA. (A) Percentage of motile cells. (B) Percentage progressive motility. (C-D) Representative sperm tracks from control and *Aurka* spcKO sperm. (E) Path velocity (VAP), progressive velocity (VSL), track speed (VCL), relative motility index, (RMI = % motility X VSL)/100), were all increased in the *Aurka* spcKO sperm, with VAP, VCL, and RMI significant at $P \leq 0.02$, and VSL not statistically significant at $P = 0.06$. Other parameters including lateral amplitude (ALH), beat frequency (BCF), straightness (STR), and linearity (LIN) were not significantly different in *Aurka* spcKO sperm compared to controls.

Table 2. ***AURKA was associated with specific fibrous sheath proteins, cytoskeletal proteins, mitochondrial proteins, and metabolic proteins.*** AURKA was immunoprecipitated from sperm lysates with an AURKA-specific antibody. On-bead digestion was conducted, and co-purified proteins identified by MALDI-TOF. Fibrous sheath proteins are indicated in yellow, microtubule binding proteins in green, mitochondrial proteins in red, and metabolic enzymes in blue

Identified Proteins	ID	# peptides	# peptides control
Ribosome-binding protein 1	RRBP1	22	0
Fibrous sheath CABYR-binding protein	FSCB	15	0
Tektin-3	TEKT3	13	0
Spermatid-specific manchette-related protein 1	SMRP1	9	0
Tektin-5	TEKT5	9	0
Transport and Golgi organization protein 1 homolog	TGO1	10	0
Tektin-2	TEKT2	10	0
Sperm equatorial segment protein 1	SPESP	7	0
Zonadhesin	ZAN	9	0
A-kinase anchor protein 4	AKAP4	9	0
Serine/threonine-protein phosphatase PGAM5, mitochondrial	PGAM5	7	0
Phosphoglycerate kinase 2	PGK2	6	0
Dihydrolipoyllysine-residue acetyltransferase component of pyruvate dehydrogenase complex, mitochondrial	ODP2	7	0
EF-hand domain-containing protein 1	EFHC1	8	0
Clusterin	CLUS	7	0
Dynein heavy chain 8, axonemal	DYH8	7	0
Outer dense fiber protein 3	ODF3A	7	0
Calcium-binding tyrosine phosphorylation-regulated protein	CABYR	7	0
Fibronectin	FINC	5	0
Nucleoside diphosphate kinase 7	NDK7	6	0
von Willebrand factor A domain-containing protein 8	VWA8	6	0
EF-hand domain-containing family member C2	EFHC2	6	0
Protein FAM166A	F166A	6	0

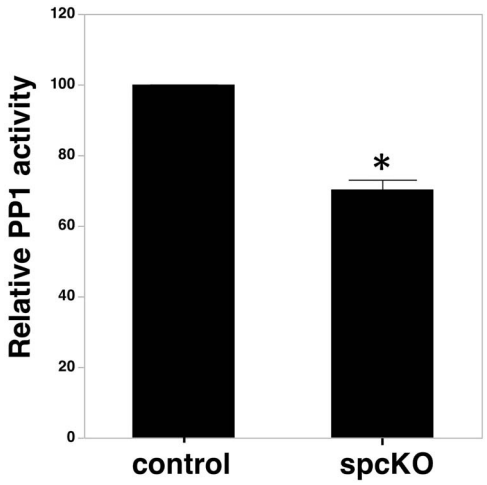

Figure 9. ***PP1 activity was reduced in Aurka spcKO sperm.*** Sperm lysates were prepared from *Aurka* spcKO and control sperm and the activity of PP1 in the *Aurka* spcKO lysate relative to that in control lysate is shown. N = 3 each for *Aurka* spcKO and control. Error bars equal SEM, P = 0.0004.

Table 3. ***Predicted AURKA phosphorylation sites.*** The sequence of each of the listed proteins was analyzed for potential high confidence AURKA phosphorylation sites using a kinase-specific phosphorylation site prediction program, GPS 5.0. A portion of each sequence is shown containing the phosphorylated serine or threonine in red

Protein	Site	Sequence
AKAP4	225	SFYVNRL*S*SLVIQMA
	497	LTSAERV*S*EHILKES
CAYBR	120	PLFSNKT*T*QFPSVHA
	357	ENSQHKS*S*VHVEAEA
FSCB	25	YRRRRRP*S*QPMVDKS
PGK2	8	MALSAKL*T*LDKVDLK
DHC8	141	RPSKFRR*S*MTGIPNL
	527	NTSERMT*S*LFIKVTN
TEK2	320	LAHTRLE*S*RTYRSNV
TEK3	117	SNSSRHN*S*ERLRVDT
TEK5	348	LAFNARI*S*EETDVKN
ATP5C1	6	MFSRA*S*VVGLSAC
	255	SEQSARM*T*AMDNASK
PPP1CC2	22	RLLEVRG*S*KPGKNVQ
	100	YVDRGKQ*S*LETICLL
	311	PNATRPV*T*PPRVGSG
PPP1R2	23	KNKTSAA*S*PPVVPSA
	194	EESSQGS*T*TSDHLQH
	195	ESSQGST*T*SDHLQHK

phosphorylating downstream targets on the centrosome and kinetochore to regulate spindle formation, chromosome segregation and mitotic entry [20–24]. Using two different lines of Cre-expressing mice, here we identified distinct requirements for AURKA in male germ cell mitotic and meiotic cell divisions during spermatogenesis as well as for normal sperm development and motility. AURKA is a component of the flagellar midpiece and principal piece, and we identified AURKA-interacting partners that are constituents of the mitochondria, fibrous sheath, and axoneme of the sperm flagellum

that represent excellent candidate substrates of AURKA to control sperm motility.

AURKA is abundantly expressed in postmeiotic germ cells

AURKA protein was undetectable in dividing spermatogonia becoming most abundant in spermatids (Figure 1). This was a surprising finding given the known role for AURKA in cell division. In contrast our data show that AURKA is localized to developing spermatids (Figure 2) and is expressed in spermatids during the first wave of spermatogenesis (Figure 1). Previously we have detected AURKA in spermatogonia, due likely to different incubation conditions and the distinct epitopes of the antibodies used. Our results that *Aurka* deletion in spermatogonia eliminated the germ line revealed it must be expressed in either prospermatogonia or spermatogonia; it may be that it is localized to spindle poles at a level that is undetectable by immunofluorescence under our conditions. Studies using single-cell RNAseq found that AURKA is expressed in spermatogonia [25] and spermatocytes [26, 27] consistent with a role for this protein in mitosis and meiosis.

Our results are strikingly different from that of the Jordan group whose findings were reported while this manuscript was in review (Wellard et al. [28]); they found that the primary defect in their spermatocyte specific knockout animals occurs in meiosis not in spermatids. We believe that the major cause of the discrepancy between our results and theirs is that Dr. Jordan's group chose to use the *Spo11*-cre transgene to produce their spermatocyte specific KOs [29] and the absence of data verifying the time at which recombination occurs. The *Spo-11* transgene, which is present in multiple copies in the transgenic mouse, contains the entire genomic locus of the *Spo11* gene not just the promoter with approximately 5 kb sequence upstream of the start site fused to an IRES/GFP/Cre cassette. Importantly, SPO11 catalyzes double-strand breaks (DSBs) to initiate meiotic recombination. The activity of SPO11 is regulated by negative feedback resulting in a significant decrease in SPO11 in transgenic animals, which has direct and substantial effects on meiotic progression [30]. Reduced levels of this protein leads to delayed synapsis, pachytene arrest, apoptosis, reduced testis size, and infertility [31] strikingly similar to the phenotypes described in the Jordon paper. In addition, *Spo11* mRNA has been detected at P7, a time when stem cells, progenitors, and differentiating spermatogonia are found [32]. Indeed, the only time point that has been determined for Cre expression from this transgene was taken at P10 [32]. The Wellard et al. manuscript did not verify the time at which recombination occurs in their animals that we have precisely demonstrated here to occur beginning at p16 at a time significantly later than the timing of expression of *Spo11* (Figure 5A). Neither did they verify their knockout by western blot. Recombination of the deleted allele has not been reported in other studies, to our knowledge. Taken together these facts support our conclusion that AURKA functions in developing spermatids, a novel finding. In fact, this suggests that the results from the many studies using this transgene should be reevaluated.

AURKA is required for mitosis in male germ cells

As expected, based upon its critical role in mitosis, deletion of *Aurka* in spermatogonia resulted in loss of the germline in *Aurka* spgKO animals (Figure 4), presumably due to a block in mitosis. Deletion of *Aurka* in spermatocytes resulted in animals with testis significantly smaller than controls, and a significant reduction in sperm count although they had an apparently normal distribution of cell types in the adult testis (Figure 5, H-H′). This latter defect resulting from deletion in spermatocytes was manifested as a reduction in fertility (Figure 5D). The observation that mice were not infertile and that *Aurka* spcKO mutant seminiferous tubules contained meiotic cells is intriguing; this could result from partial compensation for AURKA by AURKC in meiosis. AURKA is a member of a small family of related kinases with disparate localization and functions in mitosis [13, 33]. AURKA is located at centrosomes, spindle fibers near centrosomes, and to the midbody at cytokinesis [34, 35], and mutations in AURKA result in monopolar spindles [36]. Although its primary role is in mitosis, AURKA plays a role in progression through meiosis through stimulating transcription of *Mos*, a germ cell-specific kinase responsible for activation of the MAPK pathway necessary for progression through meiosis [13, 37].

Less is known about AURKC, which is highly expressed in pachytene spermatocytes and oocytes and is required for spermatogenesis and for progression through meiosis in oocytes [38–42]. AURKC has a known role in meiosis in male germ cells in the mouse [42, 43]. Both isoforms are localized at spindle poles [44, 45] and AURKA is known to compensate for loss of AURKC in mouse oocytes [44]. Like AURKA, a portion of AURKC is also found at spindle poles [46]. In addition, AURKC is regulated by the kinase haspin which is required for MTOC clustering in mouse oocytes. We speculate that these overlapping localizations and functions in formation of the spindle may allow AURKC to compensate for loss of AURKA in male germ cells. The incomplete compensation is manifest in the increased apoptosis observed in spermatocytes (Figure 5). This possibility will be addressed in future studies by testing the genetic interaction of these related kinases using AURKA/AURKC double knockout mice [40, 47].

AURKA is important for normal sperm morphology and motility

Testes of *Aurka* spcKO mice produced large numbers of morphologically abnormal sperm, which contained multiple and bent flagella and malformed heads (Figure 7 E-I). Notably, mutations in AURKC also caused defects in sperm morphology. A genome-wide microsatellite screen of 14 infertile men with large-headed sperm (macrozoospermia) and multiple flagella revealed that affected individuals harbored a nonsense mutation in the *Aurkc* gene that truncated most of the kinase catalytic domain of this kinase [41]. Furthermore, *Aurkc*-null mice had malformed heads and acrosomes with uncondensed chromatin [40]. Our result here that *Aurka* deletion in spermatocytes causes malformed sperm along with the possible compensation of AURKC for AURKA suggests a mechanistic overlap of aurora kinase function in spermatogenesis [48, 49]. Completion of meiosis requires successful separation of daughter cells at cytokinesis. We have localized AURKA to the contractile ring prior to abscission in mitotically dividing cells [50]. In addition, AURKA is required for high-fidelity cytokinesis in *Drosophila* and its overexpression in cells lacking TRP53 causes tetraploidization [51]. Deletion of AURKA in spermatocytes could result in abnormal haploid gametes.

Caudal epididymal sperm lacking AURKA surprisingly displayed increased progressive motility (Figure 8). Progressive motility is initiated in the cauda epididymis by inhibition of PP1CC2 activity by PPP1R2 which in turn is regulated by GSK3A [6, 52, 53]. We propose that PPP1R2 is a potential target of AURKA. Loss of AURKA would be predicted to decrease phosphorylation of PPP1R2, with increased binding and inhibition of PP1 activity resulting in increased sperm motility. This is consistent with the reduction in PP1 activity in

Aurka spcKO sperm (Figure 9) and we are currently investigating whether PPP1R2 is direct target of AURKA action in the epididymis. In fact, the 25% increase in motility of the *Aurka* spcKO sperm is comparable to the level of decrease in PP1 activity in these mice. Both PPP1R2 and PP1CC have predicted high confidence AURKA recognition sites and are therefore candidate targets of this kinase (Table 3).

Mitochondrial proteins and metabolic proteins are AURKA binding partners

Consistent with the localization of AURKA to the midpiece of the flagellum (Figure 7C-C'), the most abundant class of proteins found associated with AURKA are mitochondrial proteins (Table 1). Although this finding is unexpected, it is not unprecedented. A recent report identified AURKA as a mitochondrial protein in cancer cells and in *Drosophila* [54]. Mitochondrial AURKA regulates mitochondrial connectivity and ATP production [54, 55]. Overexpression of AURKA in this system increased complex IV abundance and ATP production. Furthermore, AURKA has a cryptic mitochondrial localization signal [55]. Interestingly, components of the electron transport chain, including the complex IV subunits F_0 and F_1 ATPase, were found associated with AURKA in sperm flagella lysate. Both ATP5b and ATP5c1, subunits of the F_0 and F_1 ATPase, respectively, are high-confidence substrates of AURKA.

Proteins of the fibrous sheath are potential targets of AURKA

AURKA associates with proteins of the fibrous sheath and axoneme, including calcium- and microtubule-binding proteins (Tables 1 and 2). In other studies, targeted deletion of many of these proteins reduced sperm motility and disrupted flagellar structure, resulting in reduced fertility or infertility [56]. Two important calcium-binding proteins, FSCB and CABYR, were identified in our screen (Table 2). Both reside on the fibrous sheath and are required for its formation and integrity [57, 58]. CABYR knockouts are severely subfertile, and their sperm had reduced motility [56, 59, 60]. We also identified the scaffolding protein AKAP4 as an AURKA binding protein. AKAP4 is the most abundant protein of the fibrous sheath and anchors PKA in an ideal position to regulate proteins important for motility [61]. PKA anchoring proteins are known to act as signaling scaffolds for multiple phosphatases and kinases in addition to PKA [62]. Deletion of AKAP4 disrupted the fibrous sheath and causes infertility [59, 60]. Our finding that AURKA is a binding partner of AKAP4 links it to the PKA signaling pathway [62]. We predict that AKAP4 localizes AURKA near its substrate proteins on the fibrous sheath so these two kinase classes can coordinately regulate motility.

Tektins and dynein of the flagellar axoneme are AURKA binding partners

In addition to proteins of the fibrous sheath, we also identified AURKA binding partners in the sperm axoneme. These include members of the tektin family of microtubule stabilizing proteins [63, 64] and the molecular motor dynein heavy chain 8 (DNAH8). TEKT2-deficient mice display an array of infertility phenotypes [65, 66]. AURKA also associates with an axonemal dynein isoform, a member of the class of molecular motors that powers flagellar bending and is regulated by calcium [67]. Mutations in axonemal dynein heavy chain isoform 8 (DNAH8) are associated with asthenozoospermia in human patients [68]. Importantly, each of these proteins has predicted high confidence AURKA phosphorylation sites (Table 3) [69]. We propose that AURKA, positioned on the fibrous sheath by AKAP4, phosphorylates proteins of the axoneme to control sperm motility.

Summary

Here, we demonstrate a requirement for AURKA in survival of mitotic spermatogonia, maintenance of spermatocytes, and spermatid morphogenesis. Furthermore, we show that AURKA regulates sperm motility likely through regulation of PP1 activity, as well as a possible role in a signaling pathway regulating sperm motility in the epididymis. AURKA is found on the midpiece of the sperm flagellum and is associated with mitochondrial proteins. Additionally, AURKA associates with key proteins of the fibrous sheath and axoneme that are critical for normal sperm structure and function. The AURKA binding proteins we identified here represent potential AURKA phosphorylation targets that expand our repertoire of known components of the apparatus directing sperm motility.

Supplementary material

Supplementary material is available at *BIOLRE* online.

Data availability

The data underlying this article will be shared on reasonable request to the corresponding author.

Author contributions

BH conducted the CASA analysis. WCL and BE maintained the breeding colony and NS performed H&E staining of mutant and control testis. TJ performed the apoptosis assay and colocalized AURKA and germ cell markers in the testis, and AOS and CBG conceived and designed the experiments and wrote the manuscript.

Acknowledgements

The authors thank Drs. Cowley and Warman for their help in designing primers to characterize the mouse lines. In addition, Dr. Warman, who generated the *Wisp3*-Cre used in this study, provided invaluable assistance in designing the experiment to determine the timing of *Aurka* deletion in our spcKO.

Funding

This work was supported by grants R15HD08015 (A.O.S) and R01HD090083 (C.B.G) from the National Institute of Child Health and Human Development. Proteomic analysis was performed using the UNC Proteomics Core Facility, which is supported in part by grant P30 from the National Cancer Institute to the UNC Lineberger Comprehensive Cancer Center.

Conflicts of Interest: The authors declare no conflict of interest.

References

1. Fawcett DW. The mammalian spermatozoon. *Dev Biol* 1975; **44**:394–436.

2. Nikonova AS, Astsaturov I, Serebriiskii IG, Dunbrack RL Jr, Golemis EA. Aurora a kinase (AURKA) in normal and pathological cell division. *Cell Mol Life Sci* 2013; **70**:661–687.
3. Luo M, Cao M, Kan Y, Li G, Snell W, Pan J. The phosphorylation state of an aurora-like kinase marks the length of growing flagella in Chlamydomonas. *Curr Biol* 2011; **21**:586–591.
4. Pugacheva EN, Jablonski SA, Hartman TR, Henske EP, Golemis EA. HEF1-dependent aurora a activation induces disassembly of the primary cilium. *Cell* 2007; **129**:1351–1363.
5. Johnson ML, Wang R, Sperry AO. Novel localization of aurora a kinase in mouse testis suggests multiple roles in spermatogenesis. *Biochem Biophys Res Commun* 2018.
6. Freitas MJ, Vijayaraghavan S, Fardilha M. Signaling mechanisms in mammalian sperm motility. *Biol Reprod* 2017; **96**:2–12.
7. Cowley DO, Rivera-P√©rez JA, Schliekelman M, He YJ, Oliver TG, Lu L, O'Quinn R, Salmon ED, Magnuson T, Van Dyke T. Aurora-a kinase is essential for bipolar spindle formation and early development. *Mol Cell Biol* 2009; **29**:1059–1071.
8. Busada JT, Kaye EP, Renegar RH, Geyer CB. Retinoic acid induces multiple hallmarks of the prospermatogonia-to-spermatogonia transition in the neonatal mouse. *Biol Reprod* 2014; **90**:64.
9. Busada JT, Velte EK, Serra N, Cook K, Niedenberger BA, Willis WD, Goulding EH, Eddy EM, Geyer CB. Rhox13 is required for a quantitatively normal first wave of spermatogenesis in mice. *Reproduction* 2016; **152**:379–388.
10. Goodson SG, Zhang Z, Tsuruta JK, Wang W, O'Brien DA. Classification of mouse sperm motility patterns using an automated multiclass support vector machines model. *Biol Reprod* 2011; **84**:1207–1215.
11. Serra N, Velte EK, Niedenberger BA, Kirsanov O, Geyer CB. The mTORC1 component RPTOR is required for maintenance of the foundational spermatogonial stem cell pool in mice. *Biol Reprod* 2018.
12. Youn JY, Dunham WH, Hong SJ, Knight JDR, Bashkurov M, Chen GI, Bagci H, Rathod B, MacLeod G, Eng SWM, Angers S, Morris Q et al. High-density proximity mapping reveals the subcellular organization of mRNA-associated granules and bodies. *Mol Cell* 2018; **69**:517–532 e511.
13. Crane R, Gadea B, Littlepage L, Wu H, Ruderman JV. Aurora a, meiosis and mitosis. *Biol Cell* 2004; **96**:215–229.
14. Lu LY, Wood JL, Ye L, Minter-Dykhouse K, Saunders TL, Yu X, Chen J. Aurora a is essential for early embryonic development and tumor suppression. *J Biol Chem* 2008; **283**:31785–31790.
15. Gallardo T, Shirley L, John GB, Castrillon DH. Generation of a germ cell-specific mouse transgenic Cre line, vasa-Cre. *Genesis* 2007; **45**: 413–417.
16. Hann S, Kvenvold L, Newby BN, Hong M, Warman ML. A Wisp3 Cre-knockin allele produces efficient recombination in spermatocytes during early prophase of meiosis I. *PLoS One* 2013; **8**:e75116.
17. Huangda W, Sherman BT, Lempicki RA. Systematic and integrative analysis of large gene lists using DAVID bioinformatics resources. *Nat Protoc* 2009; **4**:44–57.
18. Huangda W, Sherman BT, Lempicki RA. Bioinformatics enrichment tools: Paths toward the comprehensive functional analysis of large gene lists. *Nucleic Acids Res* 2009; **37**:1–13.
19. Wang C, Xu H, Lin S, Deng W, Zhou J, Zhang Y, Shi Y, Peng D, Xue Y. GPS 5.0: An update on the prediction of kinase-specific phosphorylation sites in proteins. *Genomics Proteomics Bioinformatics* 2020; **18**:72–80.
20. Kinoshita K, Noetzel TL, Pelletier L, Mechtler K, Drechsel DN, Schwager A, Lee M, Raff JW, Hyman AA. Aurora a phosphorylation of TACC3/maskin is required for centrosome-dependent microtubule assembly in mitosis. *J Cell Biol* 2005; **170**:1047–1055.
21. Seki A, Coppinger JA, Jang CY, Yates JR, Fang G. Bora and the kinase aurora a cooperatively activate the kinase Plk1 and control mitotic entry. *Science* 2008; **320**:1655–1658.
22. Kunitoku N, Sasayama T, Marumoto T, Zhang D, Honda S, Kobayashi O, Hatakeyama K, Ushio Y, Saya H, Hirota T. CENP-A phosphorylation by aurora-a in prophase is required for enrichment of aurora-B at inner centromeres and for kinetochore function. *Dev Cell* 2003; **5**: 853–864.
23. Joukov V, Walter JC, De Nicolo A. The Cep192-organized aurora A-Plk1 cascade is essential for centrosome cycle and bipolar spindle assembly. *Mol Cell* 2014; **55**:578–591.
24. Macurek L, Lindqvist A, Lim D, Lampson MA, Klompmaker R, Freire R, Clouin C, Taylor SS, Yaffe MB, Medema RH. Polo-like kinase-1 is activated by aurora a to promote checkpoint recovery. *Nature* 2008; **455**:119–123.
25. Guo J, Grow EJ, Yi C, Mlcochova H, Maher GJ, Lindskog C, Murphy PJ, Wike CL, Carrell DT, Goriely A, Hotaling JM, Cairns BR. Chromatin and single-cell RNA-Seq profiling reveal dynamic signaling and metabolic transitions during human spermatogonial stem cell development. *Cell Stem Cell* 2017; **21**:533–546 e536.
26. Wang M, Liu X, Chang G, Chen Y, An G, Yan L, Gao S, Xu Y, Cui Y, Dong J, Chen Y, Fan X et al. Single-cell RNA sequencing analysis reveals sequential cell fate transition during human spermatogenesis. *Cell Stem Cell* 2018; **23**:599–614 e594.
27. Green CD, Ma Q, Manske GL, Shami AN, Zheng X, Marini S, Moritz L, Sultan C, Gurczynski SJ, Moore BB, Tallquist MD, Li JZ et al. A comprehensive roadmap of murine spermatogenesis defined by single-cell RNA-seq. *Dev Cell* 2018; **46**:651–667 e610.
28. Wellard SR, Zhang Y, Shults C, Zhao X, McKay M, Murray SA, Jordan PW. Overlapping roles for PLK1 and aurora a during meiotic centrosome biogenesis in mouse spermatocytes. *EMBO Rep* 2021; e51023.
29. Lyndaker AM, Lim PX, Mleczko JM, Diggins CE, Holloway JK, Holmes RJ, Kan R, Schlafer DH, Freire R, Cohen PE, Weiss RS. Conditional inactivation of the DNA damage response gene Hus1 in mouse testis reveals separable roles for components of the RAD9-RAD1-HUS1 complex in meiotic chromosome maintenance. *PLoS Genet* 2013; **9**:e1003320.
30. Faieta M, Di Cecca S, de Rooij DG, Luchetti A, Murdocca M, Di Giacomo M, Di Siena S, Pellegrini M, Rossi P, Barchi M. A surge of late-occurring meiotic double-strand breaks rescues synapsis abnormalities in spermatocytes of mice with hypomorphic expression of SPO11. *Chromosoma* 2016; **125**:189–203.
31. Kauppi L, Barchi M, Lange J, Baudat F, Jasin M, Keeney S. Numerical constraints and feedback control of double-strand breaks in mouse meiosis. *Genes Dev* 2013; **27**:873–886.
32. Pellegrini M, Claps G, Orlova VV, Barrios F, Dolci S, Geremia R, Rossi P, Rossi G, Arnold B, Chavakis T, Feigenbaum L, Sharan SK et al. Targeted JAM-C deletion in germ cells by Spo11-controlled Cre recombinase. *J Cell Sci* 2011; **124**:91–99.
33. Carmena M, Earnshaw WC. The cellular geography of aurora kinases. *Nat Rev Mol Cell Biol* 2003; **4**:842–854.
34. Sugimoto K, Urano T, Zushi H, Inoue K, Tasaka H, Tachibana M, Dotsu M. Molecular dynamics of aurora-a kinase in living mitotic cells simultaneously visualized with histone H3 and nuclear membrane protein importinalpha. *Cell Struct Funct* 2002; **27**:457–467.
35. Roghi C, Giet R, Uzbekov R, Morin N, Chartrain I, Le Guellec R, Couturier A, Doree M, Philippe M, Prigent C. The Xenopus protein kinase pEg2 associates with the centrosome in a cell cycle-dependent manner, binds to the spindle microtubules and is involved in bipolar mitotic spindle assembly. *J Cell Sci* 1998; **111** (Pt 5):557–572.
36. Glover DM, Leibowitz MH, McLean DA, Parry H. Mutations in aurora prevent centrosome separation leading to the formation of monopolar spindles. *Cell* 1995; **81**:95–105.
37. Saskova A, Solc P, Baran V, Kubelka M, Schultz RM, Motlik J. Aurora kinase a controls meiosis I progression in mouse oocytes. *Cell Cycle* 2008; **7**:2368–2376.
38. Hu HM, Chuang CK, Lee MJ, Tseng TC, Tang TK. Genomic organization, expression, and chromosome localization of a third aurora-related kinase gene, Aie1. *DNA Cell Biol* 2000; **19**:679–688.
39. Yanai A, Arama E, Kilfin G, Motro B. ayk1, a novel mammalian gene related to Drosophila aurora centrosome separation kinase, is specifically expressed during meiosis. *Oncogene* 1997; **14**:2943–2950.
40. Kimmins S, Crosio C, Kotaja N, Hirayama J, Monaco L, Hoog C, van Duin M, Gossen JA, Sassone-Corsi P. Differential functions of the aurora-B and aurora-C kinases in mammalian spermatogenesis. *Mol Endocrinol* 2007; **21**:726–739.

41. Dieterich K, Soto Rifo R, Faure AK, Hennebicq S, Ben Amar B, Zahi M, Perrin J, Martinez D, Sele B, Jouk PS, Ohlmann T, Rousseaux S et al. Homozygous mutation of AURKC yields large-headed polyploid spermatozoa and causes male infertility. *Nat Genet* 2007; **39**:661–665.
42. Dieterich K, Zouari R, Harbuz R, Vialard F, Martinez D, Bellayou H, Prisant N, Zoghmar A, Guichaoua MR, Koscinski I, Kharouf M, Noruzinia M et al. The aurora kinase C c.144delC mutation causes meiosis I arrest in men and is frequent in the north African population. *Hum Mol Genet* 2009; **18**:1301–1309.
43. Tang CJ, Lin CY, Tang TK. Dynamic localization and functional implications of aurora-C kinase during male mouse meiosis. *Dev Biol* 2006; **290**:398–410.
44. Nguyen AL, Drutovic D, Vazquez BN, El Yakoubi W, Gentilello AS, Malumbres M, Solc P, Schindler K. Genetic interactions between the aurora kinases reveal new requirements for AURKB and AURKC during oocyte meiosis. *Curr Biol* 2018; **28**:3458–3468 e3455.
45. Nguyen AL, Schindler K. Specialize and divide (twice): Functions of three aurora kinase homologs in mammalian oocyte meiotic maturation. *Trends Genet* 2017; **33**:349–363.
46. Balboula AZ, Nguyen AL, Gentilello AS, Quartuccio SM, Drutovic D, Solc P, Schindler K. Haspin kinase regulates microtubule-organizing center clustering and stability through aurora kinase C in mouse oocytes. *J Cell Sci* 2016; **129**:3648–3660.
47. Wellard SR, Schindler K, Jordan P. Aurora B and C kinases regulate chromosome desynapsis and segregation during mouse and human spermatogenesis. *J Cell Sci* 2020.
48. Sharif B, Na J, Lykke-Hartmann K, McLaughlin SH, Laue E, Glover DM, Zernicka-Goetz M. The chromosome passenger complex is required for fidelity of chromosome transmission and cytokinesis in meiosis of mouse oocytes. *J Cell Sci* 2010; **123**:4292–4300.
49. Yang KT, Li SK, Chang CC, Tang CJ, Lin YN, Lee SC, Tang TK. Aurora-C kinase deficiency causes cytokinesis failure in meiosis I and production of large polyploid oocytes in mice. *Mol Biol Cell* 2010; **21**:2371–2383.
50. Bresch AM, Yerich N, Wang R, Sperry AO. The PP1 regulator PPP1R2 coordinately regulates AURKA and PP1 to control centrosome phosphorylation and maintain central spindle architecture. *BMC Mol Cell Biol* 2020; **21**:84.
51. Meraldi P, Honda R, Nigg EA. Aurora-a overexpression reveals tetraploidization as a major route to centrosome amplification in p53−/− cells. *EMBO J* 2002; **21**:483–492.
52. Vijayaraghavan S, Mohan J, Gray H, Khatra B, Carr DW. A role for phosphorylation of glycogen synthase kinase-3alpha in bovine sperm motility regulation. *Biol Reprod* 2000; **62**:1647–1654.
53. Vijayaraghavan S, Stephens DT, Trautman K, Smith GD, Khatra B, da Cruz e Silva EF, Greengard. Sperm motility development in the epididymis is associated with decreased glycogen synthase kinase-3 and protein phosphatase 1 activity. *Biol Reprod* 1996; **54**:709–718.
54. Bertolin G, Bulteau AL, Alves-Guerra MC, Burel A, Lavault MT, Gavard O, Le Bras S, Gagne JP, Poirier GG, Le Borgne R, Prigent C, Tramier M. Aurora kinase a localises to mitochondria to control organelle dynamics and energy production. *Elife* 2018; **7**.
55. Grant R, Abdelbaki A, Bertoldi A, Gavilan MP, Mansfeld J, Glover DM, Lindon C. Constitutive regulation of mitochondrial morphology by aurora a kinase depends on a predicted cryptic targeting sequence at the N-terminus. *Open Biol* 2018; **8**.
56. Young SA, Miyata H, Satouh Y, Aitken RJ, Baker MA, Ikawa M. CABYR is essential for fibrous sheath integrity and progressive motility in mouse spermatozoa. *J Cell Sci* 2016; **129**:4379–4387.
57. Li YF, He W, Jha KN, Klotz K, Kim YH, Mandal A, Pulido S, Digilio L, Flickinger CJ, Herr JC. FSCB, a novel protein kinase A-phosphorylated calcium-binding protein, is a CABYR-binding partner involved in late steps of fibrous sheath biogenesis. *J Biol Chem* 2007; **282**:34104–34119.
58. Naaby-Hansen S, Mandal A, Wolkowicz MJ, Sen B, Westbrook VA, Shetty J, Coonrod SA, Klotz KL, Kim YH, Bush LA, Flickinger CJ, Herr JC. CABYR, a novel calcium-binding tyrosine phosphorylation-regulated fibrous sheath protein involved in capacitation. *Dev Biol* 2002; **242**:236–254.
59. Miki K, Willis WD, Brown PR, Goulding EH, Fulcher KD, Eddy EM. Targeted disruption of the Akap4 gene causes defects in sperm flagellum and motility. *Dev Biol* 2002; **248**:331–342.
60. Moss SB, VanScoy H, Gerton GL. Mapping of a haploid transcribed and translated sperm-specific gene to the mouse X chromosome. *Mamm Genome* 1997; **8**:37–38.
61. Luconi M, Cantini G, Baldi E, Forti G. Role of a-kinase anchoring proteins (AKAPs) in reproduction. *Front Biosci (Landmark Ed)* 2011; **16**:1315–1330.
62. Edwards AS, Scott JD. A-kinase anchoring proteins: Protein kinase a and beyond. *Curr Opin Cell Biol* 2000; **12**:217–221.
63. Linck RW, Albertini DF, Kenney DM, Langevin GL. Tektin filaments: Chemically unique filaments of sperm flagellar microtubules. *Prog Clin Biol Res* 1982; **80**:127–132.
64. Linck R, Fu X, Lin J, Ouch C, Schefter A, Steffen W, Warren P, Nicastro D. Insights into the structure and function of ciliary and flagellar doublet microtubules: Tektins, Ca2+−binding proteins, and stable protofilaments. *J Biol Chem* 2014; **289**:17427–17444.
65. Roy A, Lin YN, Agno JE, DeMayo FJ, Matzuk MM. Tektin 3 is required for progressive sperm motility in mice. *Mol Reprod Dev* 2009; **76**:453–459.
66. Tanaka H, Iguchi N, Toyama Y, Kitamura K, Takahashi T, Kaseda K, Maekawa M, Nishimune Y. Mice deficient in the axonemal protein Tektin-t exhibit male infertility and immotile-cilium syndrome due to impaired inner arm dynein function. *Mol Cell Biol* 2004; **24**:7958–7964.
67. Smith EF. Regulation of flagellar dynein by calcium and a role for an axonemal calmodulin and calmodulin-dependent kinase. *Mol Biol Cell* 2002; **13**:3303–3313.
68. Watson CM, Crinnion LA, Morgan JE, Harrison SM, Diggle CP, Adlard J, Lindsay HA, Camm N, Charlton R, Sheridan E, Bonthron DT, Taylor GR et al. Robust diagnostic genetic testing using solution capture enrichment and a novel variant-filtering interface. *Hum Mutat* 2014; **35**:434–441.
69. Xue Y, Ren J, Gao X, Jin C, Wen L, Yao X. GPS 2.0, a tool to predict kinase-specific phosphorylation sites in hierarchy. *Mol Cell Proteomics* 2008; **7**:1598–1608.